ORIGINAL PAPER

Biogeographic differentiation between two morphotypes of the Southern Ocean diatom *Fragilariopsis kerguelensis*

Barbara Glemser[1] · Michael Kloster[1] ⬤ · Oliver Esper[1] ⬤ · Sarah Lena Eggers[1] · Gerhard Kauer[2] · Bánk Beszteri[1,3] ⬤

Abstract

Fragilariopsis kerguelensis (O' Meara) Hust. is a ubiquitous diatom of the Southern Ocean. Its thick frustules are the numerically dominant component of the siliceous sediment layer covering large parts of the seafloor beneath. Morphometric variability of frustules of this diatom has been of interest for paleoenvironmental reconstructions. Recently, two morphotypes differentiated by the morphometric descriptor rectangularity were described from a Southern Ocean sediment core, the relative abundance of which correlated with reconstructed paleotemperatures. In the present study, we use semi-automated microscopic and image analysis methods to answer whether these morphotypes also appear in recent assemblages, and if yes, do their distributions reflect geographic location or environmental factors. Three transects from the water column, sampled along the Greenwich meridian with hand nets, and one sediment surface transect from the South Pacific, were analyzed. In each of these transects, both morphotypes were detected, and annual mean sea surface temperatures (SST) were found to be a good predictor of their relative abundances. The transition between dominance of one or the other morphotype appeared roughly between the Antarctic Polar Front and the Southern Boundary of the Antarctic Circumpolar Current. Although more extensive circumpolar sampling will be needed to confirm the generality of our conclusions, the observed morphometric cline is a novel aspect of the biology of this species and can in the future potentially be used for further developing paleoproxies especially for highly *F. kerguelensis*-dominated sediment in the Southern Ocean.

Keywords *Fragilariopsis kerguelensis* · Rectangularity · Morphometrics · Biogeography

Introduction

Fragilariopsis kerguelensis (O' Meara) Hust. is an endemic diatom species of the Southern Ocean producing exceptionally strongly silicified cell walls (Scott and Thomas 2005). Due to their thickness, the frustules do not get dissolved when sinking out, unlike more fragile frustules of many other diatom species, and are thus strongly enriched in the sediment. For this reason, even though the species rarely dominates phytoplankton communities in the photic zone, its frustules commonly represent the numerically dominant component of sediment samples (Zielinski and Gersonde 1997; Cortese et al. 2004; Crosta et al. 2005; Cortese and Gersonde 2008).

Frustule morphology of the species is highly variable, and this variation repeatedly motivated attempts at taxonomic, ecological, paleoceanographic, and biomechanical-evolutionary interpretations. For instance, Frenguelli (1960) and Donahue (1971) proposed to separate varieties of *F. kerguelensis* (at the time, under the species names *Fragilariopsis antarctica* and *Nitzschia kerguelensis*, respectively). Fenner et al. (1976), in a more quantitative approach, observed morphometric trends in *F. kerguelensis* populations sampled along a meridional transect, focusing on a composite morphometric descriptor termed *F* calculated from valve length, width, and stria density. Following up, Cortese and Gersonde (2007) investigated a larger number of morphometric characters across geographically

✉ Bánk Beszteri
bank.beszteri@uni-due.de

[1] Alfred Wegener Institute Helmholtz Centre for Polar and Marine Research, Am Handelshafen 12, 27570 Bremerhaven, Germany

[2] University of Applied Sciences Emden/Leer, Constantiaplatz 4, 26723 Emden, Germany

[3] University of Duisburg-Essen, Universitätsstrasse 5, 45141 Essen, Germany

spread sediment surface samples, as well as in sediment traps and a sediment core. Their most significant observation was that average valve area of the species appeared highest in and near the Polar Frontal Zone, and it declined both towards the North and the South of this region which is considered to be the core habitat area providing good conditions to *F. kerguelensis*. This study led to several further investigations into patterns of change in *F. kerguelensis* valve area in the pelagic as well as in the sediment record. From these, a complex paleoecological interpretation framework linking trends in *F. kerguelensis* valve area with the interaction between environmental determinants (mainly temperature and iron supply) and organismal autecology emerged (Cortese et al. 2012; Shukla et al. 2013; Nair et al. 2015; Shukla and Romero 2018). Along similar lines, Crosta (2009) compared valve length distributions in *F. kerguelensis* and its congener *F. curta* in a sediment core. Finally, following the demonstration of an extremely high mechanical resistance of *F. kerguelensis* frustules (Hamm et al. 2003), Wilken et al. (2011) demonstrated correlated phenotypic plasticity in morphometric variability and biomechanics in *F. kerguelensis*.

This extensive body of research of patterns of intraspecific morphological variation in *F. kerguelensis* was recently extended by the differentiation of two valve outline shape morphological variants in a sediment core (Kloster et al. 2018). This study used semi-automated microscopic and image analysis methods for a precise morphometric characterization of *F. kerguelensis* assemblages across two glacial-interglacial transitions in the Polar Frontal Zone sediment core PS1768-8 (Zielinski et al. 1998; Gersonde et al. 2003). These analyses revealed the presence of two morphotypes distinguished by their valve rectangularity (Droop 1995). The low rectangularity morphotype (with lanceolate to rhombic valve outline shape) was present throughout the core, whereas the high rectangularity morphotype (showing more elliptic valve outlines) appeared only in samples with low reconstructed paleotemperatures (below 1 °C). The possibility was raised that the relative abundance of both morphotypes might be informative about paleoenvironmental conditions, but this hypothesis could not be tested convincingly using only fossil assemblages.

This contribution follows up on the description of these two *F. kerguelensis* morphotypes and addresses the following questions: do both morphotypes also appear in recent (water column and sediment surface) assemblages? If yes, do they show an ecological-biogeographic differentiation that might be of interest for better understanding the biology of the taxon and for paleoceanographic applications?

Material and methods

Samples from four meridional transects across different water masses of the Southern Ocean were analyzed. Three transects consisted of hand net catches from the photic zone (20 µm mesh size, depth range approx. 15–20 m to the surface) collected in the South Atlantic along the Greenwich meridian, and one of surface sediment samples from the South-East Pacific. Material was oxidized by acidic potassium permanganate treatment and mounted in Naphrax. Table 1 gives a listing of samples used (also see Fig. 1).

For data acquisition, we used a simplified variant of the workflow described in Kloster et al. (2017). Utilizing a Metafer slide scanning system (Metasystems, Altlussheim, Germany), between 36 and 369 valves per slide (Table 1) were located manually and imaged with a ZEISS Planapochromat oil immersion objective (NA = 1.4) in 20 focus depths in 0.2 µm distances, and from these focus stacks, extended focus images were calculated. The large differences in number of specimens analyzed per slide reflect the high variation in the abundance of *F. kerguelensis* valves in the investigated assemblages. We aimed to capture at least 50 valves per slide, but in three cases this was not possible due to the low number of specimens present. The obtained extended focus images were then analyzed with SHERPA (Kloster et al. 2014) to segment valve outlines and extract morphometric features, of which we focused on rectangularity. SHERPA calculates rectangularity following the approach used for diatom valves by Droop (1995), that is by dividing valve area by the area of the circumscribed rectangle lying parallel with the major axis of the valve. Further downstream data analyses were performed and all figures were created using R 3.5.1 (R Core Team 2015). Gaussian mixture models were fitted to rectangularity distributions with the *mixtools* R package (Benaglia et al. 2009). Average locations of the Southern Ocean Fronts following Orsi et al. (1995) were obtained through the *orsifronts* R package. Mean annual values of environmental conditions at the sampling locations (sea surface temperature, salinity, nitrate, and silicate concentration) were extracted from 1° resolution fields provided in World Ocean Atlas 2009 (Levitus et al. 2010). Microscopic images and data are available under https://doi.pangaea.de/10.1594/PANGAEA.896515.

Results and discussion

Altogether, 3973 specimens from 39 sampling locations along the four transects were analyzed (Table 1). Rectangularity values of individual valves ranged from 0.676 to 0.836. Rectangularity distribution for all samples pooled showed two distinct modes, albeit with slightly shifted locations and

Table 1 Samples used and their *Fragilariopsis kerguelensis* morphotype composition estimated using different approaches

Station	Cruise	Date	Lat	Lon	N	LR.mix (%)	LR.sed (%)	LR.recent (%)
PS103-1	PS103	20.12.2016	−45.954	6.287	89	100.0	93.3	97.8
PS103-2	PS103	21.12.2016	−49.014	2.837	65	98.5	92.3	96.9
PS103-3	PS103	22.12.2016	−51.993	2.099	89	93.1	85.4	93.3
PS103-4	PS103	23.12.2016	−55.878	1.056	82	22.1	19.5	23.2
PS103-5	PS103	24.12.2016	−59.047	0.078	63	1.6	1.6	1.6
PS103-6	PS103	25.12.2016	−60.000	0.000	369	0.8	0.8	1.4
PS103-7	PS103	26.12.2016	−63.000	0.064	106	1.0	0.9	3.8
PS103-9	PS103	27.12.2016	−66.001	0.004	75	5.6	5.3	6.7
PS103-11	PS103	28.12.2016	−66.538	0.001	46	2.9	4.3	6.5
PS103-12	PS103	28.12.2016	−67.029	0.001	38	18.1	18.4	18.4
PS103-14	PS103	29.12.2016	−68.012	0.006	143	26.6	23.8	27.3
PS40-35	PS40	12.04.1996	−55.000	−0.002	87	92.3	80.5	90.8
PS40-37	PS40	13.04.1996	−56.000	0.000	76	54.6	73.7	86.8
PS40-38	PS40	13.04.1996	−56.986	0.067	69	31.5	33.3	43.5
PS40-44	PS40	15.04.1996	−60.001	−0.001	89	0.0	0.0	1.1
PS40-48	PS40	16.04.1996	−61.986	0.000	86	5.2	4.7	7.0
PS40-50	PS40	17.04.1996	−63.001	0.000	89	5.6	5.6	6.7
PS40-52	PS40	18.04.1996	−64.000	−0.001	74	1.8	2.7	4.1
PS40-54	PS40	18./19.04.1996	−65.000	0.017	72	4.4	5.6	5.6
PS40-56	PS40	19.04.1996	−65.986	−0.019	71	0.0	0.0	0.0
PS40-57	PS40	20.04.1996	−66.500	0.000	82	1.5	1.2	4.9
PS40-60	PS40	21.04.1996	−68.000	0.001	91	8.0	7.7	11.0
PS40-62	PS40	21./22.04.1996	−68.986	−0.001	83	8.2	7.2	9.6
PS40-66	PS40	22./23.04.1996	−69.635	−0.118	52	5.4	5.8	5.8
PS79-38	PS79	09.12.2011	−45.108	0.004	86	100.0	96.5	98.8
PS79-39	PS79	10.12.2011	−51.452	0.003	116	99.2	93.1	97.4
PS79-40	PS79	10.12.2011	−53.502	−0.003	118	99.2	94.9	98.3
PS79-41	PS79	11.12.2011	−55.008	0.000	97	81.6	73.2	77.3
PS79-42	PS79	12.12.2011	−56.501	−0.002	97	17.1	15.5	18.6
PS79-43	PS79	12.12.2011	−58.286	0.053	111	9.0	8.1	9.9
PS79-44	PS79	14.12.2011	−64.089	−0.117	61	11.2	11.5	11.5
MUC2686	PS35	17.04.1995	−68.322	−89.627	68	44.8	33.8	44.1
MUC2688	PS35	21.04.1995	−67.217	−91.821	116	77.4	67.2	73.3
MUC2690	PS35	21.04.1995	−65.444	−90.796	327	74.3	64.8	71.3
MUC2692	PS35	22.04.1995	−65.139	−90.683	120	80.8	67.5	76.7
MUC2696	PS35	25.04.1995	−63.977	−89.541	107	90.8	79.4	88.8
MUC2697	PS35	26.04.1995	−62.997	−89.493	138	93.3	84.8	92.0
MUC2699	PS35	28.04.1995	−61.018	−89.499	107	90.0	86.9	87.9
MUC2701	PS35	30.04.1995	−59.441	−89.506	119	87.5	78.2	84.0

Lat decimal latitude; *Lon* decimal longitude; *N* number of valves analyzed. *LR.mix* proportion of valves assigned to the low rectangularity morphotype by fitting a two-component Gaussian mixture to the sample distribution of rectangularity values. *LR.sed* proportion of low rectangularity morphotype estimated using the threshold based on sediment data from Kloster et al. (2018; threshold 0.761). *LR.recent* proportion of low rectangularity morphotype estimated using the threshold based on the present data set (threshold 0.753)

differing relative contributions when compared to previous observations from the sediment record (Kloster et al. 2018) (Fig. 2). The two types of valve morphologies are illustrated in Fig. 2 and 9 in Kloster et al. (2018). For comparison with the results of Kloster et al. (2018), a two-component normal mixture model was fitted to this distribution. This indicated (comparable values from the sediment core results from Kloster et al. 2018, given in parentheses for each parameter) that a component had a mean rectangularity of 0.73 (vs. 0.72) with a standard deviation of 0.014 (vs. 0.014) and contributed 45.9% (vs. 70% in the sediment core study). The second component had a mean of 0.79 (vs. 0.78) and
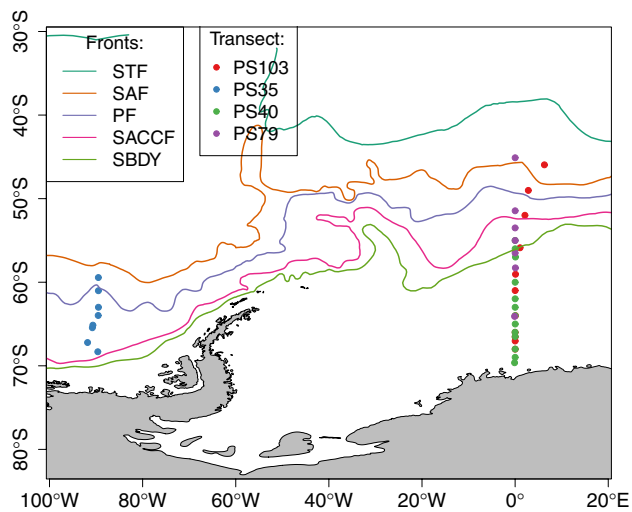
Fig. 1 Map of study area. Dots mark sampling locations color coded by transect; colored lines show the average positions of main Southern Ocean fronts following Orsi et al. (1995). Front names are abbreviated as: *STF* Subtropical Front; *SAF* Subantarctic Front; *PF* Polar Front; *SACCF* Southern ACC Front; *SBDY* Southern Boundary of the ACC. (Color figure online)
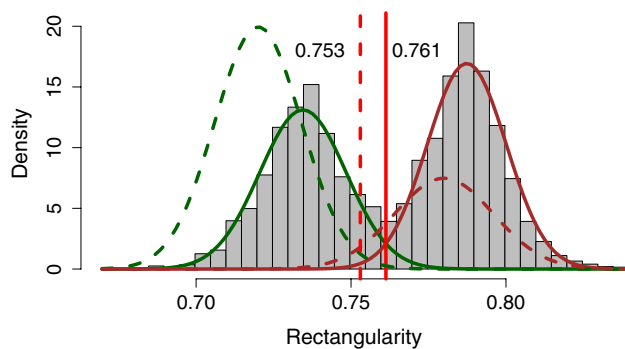

Fig. 2 Overall distribution of valve rectangularity values, and comparison between fossil and recent distributions. The histogram shows the overall rectangularity distribution pooled over all recent samples (all 39 sampling locations investigated in this study). The solid curves represent the component Gaussian distributions fitted to this data set: green, low rectangularity class, mean: (μ) 0.72, standard deviation (σ): 0.014, mixing proportion (λ): 45.9%; maroon, high rectangularity class, $\mu = 0.78$, $\sigma = 0.013$, $\lambda = 0.541$. The vertical red line indicates the point of intersection between these two normal component distributions at 0.761. For comparison, the normal component densities and their intersection point at 0.753, estimated using identical methodology from the sediment core data by Kloster et al. (2018) are plotted as dashed lines. (Color figure online)

two inferred component distributions, at 0.761. This was slightly higher than the corresponding value of 0.753 obtained by Kloster et al. (2018) from the fossil record. The location of this intersection depends not only on the mean and spread but also on the relative contributions of both component distributions. In the recent samples, the high rectangularity class contributed stronger and both rectangularity classes had slightly higher means compared to the sediment core data of Kloster et al. (2018), together explaining the difference in these threshold estimates.

To precisely estimate the relative contribution of both rectangularity classes in a particular sample, the threshold should be estimated separately for each sample; or, equivalently, a normal mixture model should be fitted to each individual sample distribution. The differences between estimates using either approach are mostly very small in this data set (Table 1, Online Resource 1), so that in practice it makes little difference which approach is used. Due to the generally expected higher precision of the mixture model-based estimates, these were used in the following analyses.

Different from the sediment core samples analyzed previously, where the contribution of the high rectangularity morphotype never exceeded 51% (Kloster et al. 2018), the relative proportion of both morphotypes varied across the full range between 0 and 100% among the recent samples investigated here. A pattern in morphotype dominance reflecting average front positions was readily visible from the individual histograms (Online Resources 2–5). The low rectangularity (lanceolate) morphotype dominated at northern sampling locations (Subantarctic Front to the polar frontal zone), often contributing 95–100% of the *F. kerguelensis* valves. South of the Antarctic Circumpolar Current (ACC), the high rectangularity (elliptic) morphotype dominated, in some cases to the complete exclusion of the low rectangularity morphotype. The transitional zone, also showing the highest variability in dominance relationships of both morphotypes, was observed between the Polar Front and the Southern Boundary of the ACC, where either morphotype could appear as dominant in the photic zone (Online Resources 2–4). In the southernmost surface sediment samples, both morphotypes were represented in relatively balanced proportions, although this transect unfortunately did not reach the Southern Boundary of the ACC (Online Resource 5).

To see if latitude could quantitatively explain this apparently shifting dominance relationship between both *F. kerguelensis* morphotypes, the contribution of the low rectangularity morphotype against latitude was plotted (Online Resource 6a). This plot indicated a clearly distinct relationship of morphotype dominance in the South Pacific compared to the three South Atlantic transects. Observing the map in Fig. 1 indicates that this distinct difference might

a standard deviation of 0.013 (vs. 0.016) and contributed the remaining 54.1% (vs. 30%) of the bimodal distribution (Fig. 2).

A threshold value of rectangularity to differentiate between both morphotypes was estimated as the intersection location between the density functions of the

be explained by the different latitudinal positions of Southern Ocean frontal systems and water masses between both ocean basins: all the ACC fronts and currents lie further South in the area of our South Pacific transect than along the Greenwich meridian where our South Atlantic transects were sampled.

Indeed, when plotting the same data (relative proportion of low rectangularity morphotype in total *F. kerguelensis* assemblage) against different environmental variables (the distribution of which reflects the circulation-driven distribution of water masses), the difference between the South Pacific and South Atlantic transects disappears (Fig. 3, Online Resource 6). This probably indicates that the relative proportion of both morphotypes is determined by the physicochemical characteristics of the water and by circulation patterns, i.e., by niche differentiation and circumpolar dispersal with ocean currents.

Some environmental factors were better correlated with the morphotype composition of *F. kerguelensis* assemblages than others: dissolved silica and salinity showed the strongest correlations among the tested untransformed environmental variables (Online Resource 6). Of these, the correlation with salinity might be irrelevant from the ecological point of view since the range in annual average salinity values considered here is rather narrow (33.8–34.4 psu). It is possible that this signals association with different surface water masses of which the salinity differences are indicative. Inspection of the scatter plot against sea surface temperature (SST) revealed a strong initial gradient in the proportion of the low rectangularity morphotype in the range below 0 °C which abruptly leveled off slightly above 0 °C (Online Resource 6b). Due to the closeness of the freezing point of seawater, it might be argued that a temperature difference of the same magnitude (e.g., 0.1 or 0.5 °C) could make a larger ecophysiological difference in the below-zero range.
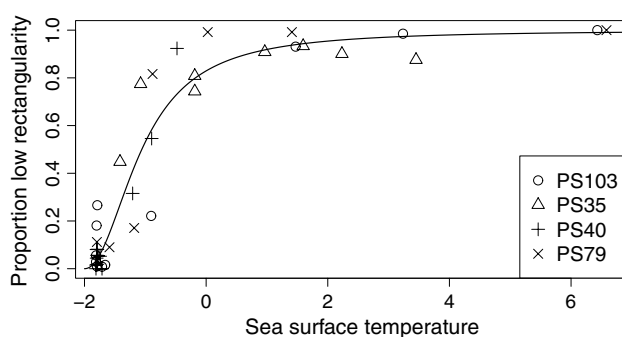
Reflecting this, a logarithmic transformation of the temperature difference from the freezing point of seawater might be a better ecological predictor variable. Indeed, the correlation of the proportion of the low rectangularity morphotype with $\log(SST + 2)$ is stronger than with any of the untransformed environmental variables (Online Resource 6c).

Observing the scatter plot of the proportion of the low rectangularity morphotype against $\log(SST + 2)$, however, reveals a non-linear relationship. Logit transformation of the dependent variable straightens out this S-shaped interrelationship. To more precisely describe this curvilinear relationship, a linear model of the form $\log\left(\frac{p}{1-p}\right) = a + b \times \log(SST + 2)$ was fitted where p is the proportion of the low rectangularity morphotype (as estimated using separately fitted mixed models to each sample distribution). This model is graphically displayed in Fig. 3. Projecting the predicted morphotype relative abundances upon an SST grid indicates that the zone of transition between dominance of the low rectangularity morphotype to the North and of the high rectangularity morphotype to the South roughly follows the Southern Boundary of the ACC (Fig. 4). Whether this dominance reversal reflects water mass distributions (ACC vs. Weddell Sea/Coastal Current, etc.), or if perhaps it might be related to winter sea ice distribution which also roughly follows the sbACC, is presently unclear, as are the biological-ecophysiological mechanisms underlying this cline.

Whereas the latter model setup reflects an autecological logic (morphotype relative abundance as a function of sea surface temperature), from the paleoceanographic point of view, the inverse relationship is of interest. In the latter setting, relative proportion of both morphotypes would be used as a predictor and an environmental variable, in this case, SST, estimated as dependent variable (Online Resource 7). This model indicated that the dominance shift from < 1 to > 99% average contribution of the low rectangularity morphotype appears in an annual mean SST range between − 1.85 and + 3.6 °C roughly between the average course of the Polar Front and the Southern Boundary of the ACC (Fig. 4). This means that the annual mean SST range in which *F. kerguelensis* morphotype relative abundance is informative about SST is roughly below + 3.6 °C, thus only making *F. kerguelensis* morphotypes a promising proxy for SST in the Southern parts of its distribution area. However, the good correspondence of the morphotype transitional zone with the location of the Southern Boundary of the ACC might make this system a good proxy for investigating past shifts in the position of this boundary front.

For completeness, we note that when extending the log-logit regression model presented in Figs. 3 and 4 to include further predictors beyond SST, annual mean nitrate concentrations showed a significant effect ($p = 2.6 \times 10^{-5}$), in
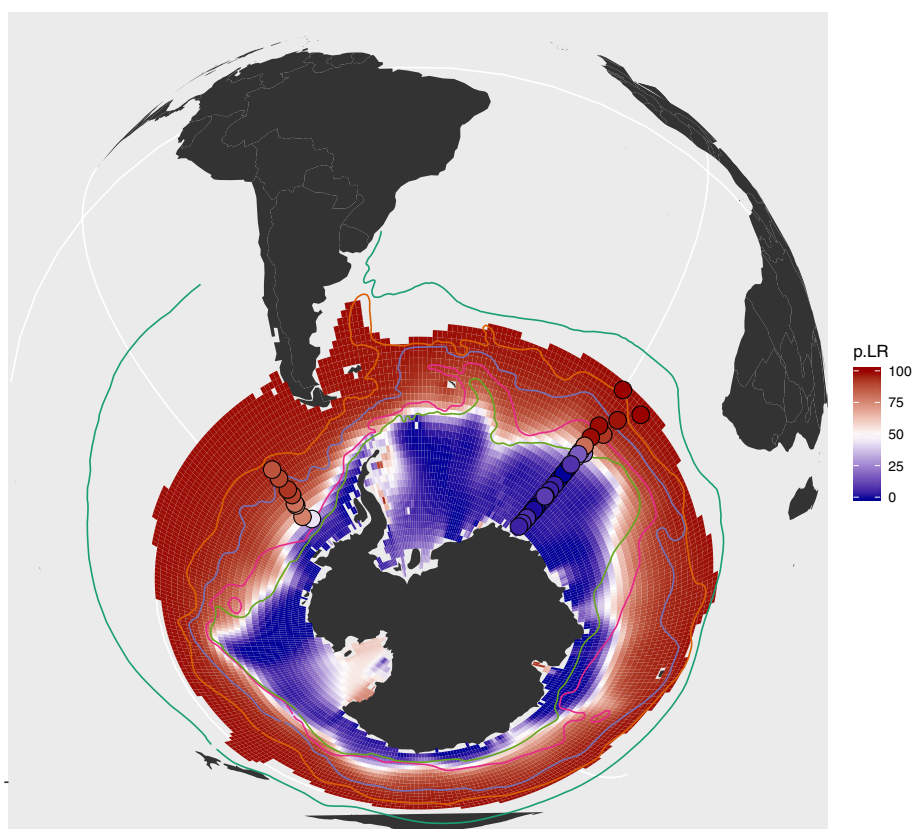

Fig. 3 Interrelationship between proportion of the low rectangularity morphotype (on the *y*-axis) and annual mean sea surface temperature (*x*-axis). The solid line represents the model $\log\left(\frac{p}{1-p}\right) = 0.125 + 2.10 \times \log(SST + 2)$ where p denotes the proportion of the low rectangularity morphotype relative to all *Fragilariopsis kerguelensis* valves in an assemblage

Fig. 4 Map illustrating the biogeographic cline between both morphotypes. Circles represent sampled stations, in color coding reflecting the percentage contribution of the low rectangularity morphotype to the *Fragilariopsis kerguelensis* assemblage (*p.LR* percent low rectangularity). Color coding of the grid shows expected relative abundance of the low rectangularity morphotype on the same scale, as inferred from annual mean sea surface temperature values using the log-logit SST model shown in Fig. 3. The Northern boundary was drawn at 7.5 °C annual mean SST, following Pinkernell and Beszteri (2014); although this is not the best available model for the Northern distribution boundary of the species, it roughly follows the latter. Color coding of the Southern Ocean fronts same as used in main Fig. 1, i.e., from North to South: turquoise—subtropical front; orange—subantarctic front; light blue—polar front; purple—Southern ACC front; grass green—Southern boundary of the ACC. (Color figure online)

contrast with silicate and salinity, which did not contribute further significant statistical signal once SST and nitrate concentrations were accounted for. It is interesting to note that nitrate concentration was also observed to be a more important predictor than silicate of *F. kerguelensis* distribution around the Northern edge of its biogeographic range (Pinkernell and Beszteri 2014). It is currently unclear whether this is more than a simple coincidence or if nitrate might in general be a better ecological-water mass predictor for Southern Ocean phytoplankton biogeography than silicate.

Before conclusions can be drawn with a high certainty and can be generalized in a circumpolar manner, however, observation of shifting morphotype dominance over geographically more broadly spread transects, and a more systematic comparison between photic zone and sediment surface assemblages, as well as between ocean basins, will be necessary. Three of the four transects investigated here came from practically the same circumpolar location, the

Greenwich meridian, and it is these transects that mainly contribute statistical signal to our inferred biogeographical-autecological model. Unfortunately, the single South Pacific transect included in our analysis does not only come from a different ocean basin, but also from the sediment surface (in contrast to all three South Atlantic transects which represent hand net samples from 20–0 m depth). The slight offset visible in the sediment transect (PS35) when compared to the water column ones (Fig. 3) is statistically significant (p = 0.02 in a log-logit analysis of covariance model with SST as continuous predictor and sediment vs. water column as grouping factor). Whether this offset reflects a biogeographic difference between the South Atlantic and the South Pacific, or is related to depositional processes (dissolution bias, transport), cannot be answered with our limited data and will need to be addressed in a more systematic manner in the future.

In light of these results, previous observations of shifting morphotype dominance in the Polar Frontal Zone

sediment core PS1768-8 (Kloster et al. 2018) can be interpreted to reflect biogeographic-oceanographic shifts during deglaciations. The fact that the contribution of the high rectangularity morphotype barely reached 50% even in the coldest glacial samples might be taken as an indication that the Southern Boundary of the ACC, although approached the core location, never shifted so far North in the investigated time slices.

The biological-taxonomic nature of the two morphotypes remains unclear even with these new data since in principle, both phenotypic plasticity and the presence of two, biogeographically differentiated taxa (semi-cryptic species) could explain our observations. Rectangularity differences between both morphotypes seem rather marked even in samples where both morphotypes co-occur. This might be more consistent with a hypothesis invoking shifting dominance relationships of two taxa: in the case of phenotypic plasticity, a more gradual transition could be expected. In order to answer this question with more confidence, however, morphometric and molecular comparison of cultured strains will be needed.

Looking at our observations in the context of previous morphometric studies makes it clear that morphometrics of *F. kerguelensis* assemblages contains rich information about environmental conditions among which these diatoms grow. Since valves of this taxon represent the dominant component of Southern Ocean siliceous sediments, this information source might warrant more attention in the future. A synthesis of accumulated information on variability in valve area (Cortese and Gersonde 2007; Cortese et al. 2012; Shukla et al. 2013; Shukla and Romero 2018), valve length (Crosta 2009), rectangularity (Kloster et al. 2018), and potentially other morphometric parameters (Fenner et al. 1976) in *F. kerguelensis* assemblages as a function of multiple environmental and oceanographic determinants seems timely. Such a synthesis will, however, require substantial further data collection, since re-analysis of previously published data sets in light of novel findings is only possible in a rather limited manner. To address this aspect, rich data supplements containing not only aggregated statistics but dozens of morphometric features extracted for each individual specimen, as well as every single specimen image, were archived both in this paper and previously by Kloster et al. (2018). We hope that these data sets can become the seed of a future, geographically, and paleoceanographically extensive data set which can be continuously extended and re-analyzed by the scientific community.

Compliance with ethical standards

References

Benaglia T, Chauveau D, Hunter D, Young D (2009) mixtools: an R package for analyzing finite mixture models. J Stat Soft 32:1–29. https://doi.org/10.18637/jss.v032.i06

Cortese G, Gersonde R (2007) Morphometric variability in the diatom *Fragilariopsis kerguelensis*: Implications for Southern Ocean paleoceanography. Earth Planet Sci Lett 257:526–544. https://doi.org/10.1016/j.epsl.2007.03.021

Cortese G, Gersonde R (2008) Plio/Pleistocene changes in the main biogenic silica carrier in the Southern Ocean, Atlantic Sector. Mar Geol 252:100–110. https://doi.org/10.1016/j.margeo.2008.03.015

Cortese G, Gersonde R, Hillenbrand CD, Kuhn G (2004) Opal sedimentation shifts in the World Ocean over the last 15 Myr. Earth Planet Sc Lett 224:509–527. https://doi.org/10.1016/j.epsl.2004.05.035

Cortese G, Gersonde R, Maschner K, Medley P (2012) Glacial-interglacial size variability in the diatom *Fragilariopsis kerguelensis*: possible iron/dust controls? Paleoceanography 27:PA1208. doi:10.1029/2011pa002187

Crosta X (2009) Holocene size variations in two diatom species off East Antarctica: productivity vs environmental conditions. Deep Sea Res Pt I 56:1983–1993. https://doi.org/10.1016/j.dsr.2009.06.009

Crosta X, Romero O, Armand LK, Pichon J-J (2005) The biogeography of major diatom taxa in Southern Ocean sediments: 2. Open ocean related species. Palaeogeogr Palaeocl 223:66–92. https://doi.org/10.1016/j.palaeo.2005.03.028

Donahue JG (1971) Diatoms as quaternary biostratigraphic and paleoclimatic indicators in high latitudes of the Pacific Ocean. Dissertation, University of Michigan

Droop S (1995) A morphometric and geographical analysis of two races of *Diploneis smithii / D. fusca* (Bacillariophyceae) in Britain. In: Marino D, Montresor M (eds) Proceedings of the thirteenth international diatom symposium. Biopress Ltd, Bristol, pp 347–69

Fenner J, Schrader HJ, Wienigk H (1976) Diatom phytoplankton studies in the southern Pacific Ocean, composition and correlation to the Antarctic convergence and its paleoecological significance. Initial Rep Deep Sea 35:757–813

Frenguelli J (1960) Diatomeas y silicoflagelados recogidas en Tierra Adelia durante las expediciones Polares Francesas de Paul Emile VICTOR (1950–1952). Rev Algol 5:3–48

Gersonde R, Abelmann A, Brathauer U, Becquey S, Bianchi C, Cortese G, Grobe H, Kuhn G, Niebler HS, Segl M, Sieger R, Zielinski U, Fütterer DK (2003) Last glacial sea surface temperatures and

sea-ice extent in the Southern Ocean (Atlantic-Indian sector): A multiproxy approach. Paleoceanography 18:1061. https://doi.org/10.1029/2002pa000809

Hamm CE, Merkel R, Springer O, Jurkojc P, Maier C, Prechtel K, Smetacek V (2003) Architecture and material properties of diatom shells provide effective mechanical protection. Nature 421:841–843. https://doi.org/10.1038/nature01416

Kloster M, Kauer G, Beszteri B (2014) SHERPA: an image segmentation and outline feature extraction tool for diatoms and other objects. BMC Bioinf 15:218. https://doi.org/10.1186/1471-2105-15-218

Kloster M, Esper O, Kauer G, Beszteri B (2017) Large-scale permanent slide imaging and image analysis for diatom morphometrics. Appl Sci 7:330. https://doi.org/10.3390/app7040330

Kloster M, Kauer G, Esper O, Fuchs N, Beszteri B (2018) Morphometry of the diatom *Fragilariopsis kerguelensis* from Southern Ocean sediment: High-throughput measurements show second morphotype occurring during glacials. Mar Micropaleontol 143:70–79. https://doi.org/10.1016/j.marmicro.2018.07.002

Levitus S et al. (2010) World Ocean Atlas 2009 vol 68-71. NOAA Atlas NESDIS. U.S. Government Printing Office, Washington, D.C.

Nair A, Mohan R, Manoj M, Thamban M (2015) Glacial-interglacial variability in diatom abundance and valve size: implications for Southern Ocean paleoceanography. Paleoceanography 30:1245–1260. https://doi.org/10.1002/2014PA002680

Orsi AH, Whitworth T, Nowlin WD (1995) On the meridional extent and fronts of the Antarctic Circumpolar Current. Deep Sea Res Pt I 42:641–673. https://doi.org/10.1016/0967-0637(95)00021-W

Pinkernell S, Beszteri B (2014) Potential effects of climate change on the distribution range of the main silicate sinker of the Southern Ocean. Ecol Evol 4:3147–3161. https://doi.org/10.1002/ece3.1138

R Core Team (2015) R: a language and environment for statistical computing. R Foundation for Statistical Computing, Vienna, Austria

Scott FJ, Thomas DP (2005) Diatoms. In: Scott FJ, Marchant HJ (eds) Antarctic marine protists. ABRS, Canberra and AAD, Hobart, Canberra, pp 13–201

Shukla SK, Romero OE (2018) Glacial valve size variation of the Southern Ocean diatom *Fragilariopsis kerguelensis* preserved in the Benguela Upwelling System, southeastern Atlantic. Palaeogeogr Palaeocl 499:112–122. https://doi.org/10.1016/j.palaeo.2018.03.023

Shukla SK, Crosta X, Cortese G, Nayak GN (2013) Climate mediated size variability of diatom *Fragilariopsis kerguelensis* in the Southern Ocean. Quaternary Sci Rev 69:49–58. https://doi.org/10.1016/j.quascirev.2013.03.005

Wilken S et al (2011) Diatom frustules show increased mechanical strength and altered valve morphology under iron limitation. Limnol Oceanogr 56:1399–1410. https://doi.org/10.4319/lo.2011.56.4.1399

Zielinski U, Gersonde R (1997) Diatom distribution in Southern Ocean surface sediments (Atlantic sector): Implications for paleoenvironmental reconstructions. Palaeogeogr Palaeocl 129:213–250. https://doi.org/10.1016/S0031-0182(96)00130-7

Zielinski U, Gersonde R, Sieger R, Fütterer D (1998) Quaternary surface water temperature estimations: Calibration of a diatom transfer function for the Southern Ocean. Paleoceanography 13:365–383. https://doi.org/10.1029/98PA01320